



Synthesis, characterization and NLO properties of a new 3D coordination polymer assembled from *p*-aminobenzoic acid

Li Li^{a,c}, Daofeng Sun^a, Zhengping Wang^b, Xinyu Song^a, Sixiu Sun^{a,*}

^a Department of Chemistry, Shandong University, 27 Shanda Nanlu, Jinan, Shandong 250100, PR China

^b State Key Lab of Crystal Materials, Shandong University, Jinan, Shandong 250100, PR China

^c College of Chemistry and Chemical Engineering, Ningxia University, Yinchuan, Ningxia 750021, PR China

ARTICLE INFO

Article history:

Received 7 October 2008

Received in revised form

2 January 2009

Accepted 5 February 2009

Available online 13 February 2009

Keywords:

NLO property

p-Aminobenzoic acid

Coordination polymer

ABSTRACT

Reaction of $\text{Zn}(\text{NO}_3)_2 \cdot 6\text{H}_2\text{O}$ with *p*-aminobenzoic acid in a 1:2 molar ratio under ethanol medium at room temperature affords a new three dimensional (3D) coordination polymer $[\text{Zn}(\text{PABA})_2] \cdot \text{H}_2\text{O}$ (**1**) (PABA = *p*-aminobenzoic acid). Single-crystal X-ray diffraction reveals that **1** crystallizes in the orthorhombic system, space group $P2_12_12_1$, $a = 7.614(2)$, $b = 11.133(3)$, $c = 16.869(4)$. **1** adopts a 3D open framework with H_2O molecules in the cavities. PABA, acting as bridging ligand as well as coordinating ligand, adopts a different coordination mode to bridge Zn atoms and form the 3D supramolecular structure which is further stabilized by N–H \cdots O, O–H \cdots O hydrogen bonding and π – π stacking interactions. Powder second-harmonic generation (SHG) efficiency measurement with Nd:YAG laser (1064 nm) radiation shows that the SHG efficiency of **1** is equivalent to KDP crystal. The present work also demonstrates that the framework of **1** is retained after removal of the guest H_2O molecules, and the H_2O molecules can be reintroduced into the framework, indicating that this complex may also be used to generate porous materials.

© 2009 Elsevier Masson SAS. All rights reserved.

1. Introduction

The synthesis of coordination polymers has attracted much interest in contemporary supramolecular chemistry because coordination polymerization may lead to materials with various controllable functions such as porosity, sensing, nonlinear optical (NLO) activity, and chirality [1–7]. Based on the knowledge of the structures of the ligands and the coordination geometries of a variety of metal centers, many functional materials can be rationally designed and synthesized by choosing proper organic and inorganic portions as linkers and building blocks [8,9].

p-Aminobenzoic acid (PABA) has been extensively studied in coordination chemistry. Due to the richness of its coordination modes (either in monodentate or chelating or bridging fashion), PABA can form complexes with various metal ions. For example, it can act as a monodentate ligand through the amine group or carboxylic acid [10–12]; deprotonated PABA ligand can act as chelating or bridging ligands through its amide or carboxylated groups [13–15]; and it may be protonated to form organic cation templating agents [16]. With the aim of preparing new materials with second-order NLO properties, we designed and synthesized

a new NLO active coordination polymer constructed from PABA and Zn^{II} , $[\text{Zn}(\text{PABA})_2] \cdot \text{H}_2\text{O}$ (**1**). As we all know, a material with second-order nonlinearity must have large molecular hyperpolarizability and crystallize in noncentrosymmetry. Molecules consist of π -electron conjugated moiety substituted by an electron donor group on one end of the conjugated structure and an electron acceptor group on the other end, forming a “push–pull” conjugated structure can meet this request. Meanwhile, the second-order nonlinear behavior in molecules can be increased and optimized by manipulation of the length and nature of the conjugated π -electron systems and the donor/acceptor strengths of end groups [17]. PABA, which is centrosymmetric yields excellent chiral coordination compound when it is coordinated to Zn^{II} . **1** adopts a 3D open framework with H_2O molecules in the cavity. PABA molecules act as bridging ligand as well as coordinating ligand. Due to the charge transfer between the donor, acceptor and metal center, **1** exhibits SHG efficiency.

2. Experimental section

2.1. Materials and general methods

All of the starting materials and solvents for synthesis were obtained commercially and used as received. Carbon, hydrogen,

* Corresponding author. Tel.: +86 531 8836 4879; fax: +86 531 8856 446.
E-mail address: ssx@sdu.edu.cn (S. Sun).

and nitrogen analyses were performed on a Vario EL III element analyzer. FTIR spectrum (KBr pellet) was taken on a Bruker vector-22 spectrometer. Differential scanning calorimetry and thermal gravity analysis (DSC/TGA) were carried out from room temperature to 600 °C using a TA Instruments SDT Q600 under N₂ atmosphere at a heating rate of 10 K min⁻¹. The intensity data were collected on a Bruker-Nonius SMART APEX II CCD diffractometer (graphite-monochromated Mo K α radiation. $\lambda = 0.71073$ Å). The structure of the crystal was solved by direct method using SHELXL program [18]. The final refinement was performed by full matrix-least-squares methods with anisotropic thermal parameters for all of the nonhydrogen atoms on F^2 . The powder X-ray diffraction patterns were recorded on a Japan Rigaku D/max- γ A 200 X-ray diffractometer by using Cu K α radiation ($\lambda = 1.5418$ Å). Kurtz powder method was used to test the NLO property of the new compound.

2.2. Synthesis of complex [Zn(PABA)₂] \cdot H₂O (**1**)

PABA (0.274 g, 2 mmol) was dissolved in boiling water (10 mL). The pH value of the above solution was adjusted to 7 by using NaOH solution (1 mol l⁻¹). Then, Zn(NO₃)₂ \cdot 6H₂O (0.297 g, 1 mmol) in ethanol solution (20 ml) was slowly added to the above solution under reflux condition. The reaction mixture was filtered and left to stand at room temperature. Light-yellow prism single crystals suitable for X-ray analysis were obtained after several days by slow evaporation of the solvent. Yield: 0.11 g. Found: C, 46.20; N, 7.85; H, 3.84. Calcd. C, 47.24; N, 7.87; H, 3.94. IR (KBr, cm⁻¹): 3428(m), 3130(m), 1615(s), 1594(s), 1569(s), 1514(m), 1437(w), 1383(s), 1325(w), 1166(w), 1124(s), 1018(w), 857(m), 779(s), 700(m), 626(m), 518(w), 445(w).

3. Results and discussion

3.1. Crystal structure

A summary of the crystallographic data and structure refinement is listed in Table 1. Selected bond distance and bond angle data are summarized in Table 2. X-ray crystallography reveals that **1** crystallizes in the orthorhombic system, space group $P2_12_12_1$. The asymmetric unit of **1** is presented in Fig. 1(a). As depicted in Fig. 1(b), zinc center is five coordinated by three O atoms and two N atoms

Table 1
Crystallographic data and structure refinement summary for [Zn(PABA)₂] \cdot H₂O.

Empirical formula	C ₁₄ H ₁₄ N ₂ O ₅ Zn
Formula weight	355.64
Crystal size (mm)	0.5 \times 0.2 \times 0.2
Temperature	298(2)
Crystal system	Orthorhombic
Space group	$P2_12_12_1$
<i>a</i> (Å)	7.6145(2)
<i>b</i> (Å)	11.1330(3)
<i>c</i> (Å)	16.8688(4)
beta(deg)	90.00
Volume (Å ³)	1430.01(6)
<i>Z</i>	4
<i>D</i> _{calcd} (g cm ⁻³)	1.652
μ (mm ⁻¹)	1.743
<i>F</i> (000)	728
Range of <i>h, k, l</i>	-8/9, -13/13, -20/21
Total reflections	2931
Independent reflections	1895
Parameters	203
<i>R</i> indices [<i>I</i> > 2 σ (<i>I</i>)]	0.0565, 0.1462
<i>R</i> (all data)	0.0987, 0.1669
Goodness of fit on <i>F</i> ²	0.972

Table 2
Selected bond distances and angles for [Zn(PABA)₂] \cdot H₂O.

Moiety	Distance (Å)	Moiety	Distance (Å)
Zn–O2	2.487(5)	Zn–O1	1.979(5)
Zn–O3	1.942(5)	Zn–N2	2.078(7)
Zn–N1	2.079(6)		
Moiety	Angle (deg)	Moiety	Angle (deg)
O1–Zn–O2	57.72(19)	O3–Zn–O1	112.9(2)
N2–Zn–N1	117.3(3)	O1–Zn–N2	102.6(2)
O3–Zn–N1	100.4(3)	N2–Zn–O2	82.6(2)
O4–C8–O3	124.0(7)	O1–C1–C2	119.4(7)

from four different PABA ligands, one of which is chelate coordinated through COO⁻ and others are monodentated coordinated through N or O atoms, with the bond distance $d(\text{Zn–O1}) = 1.979$ Å, $d(\text{Zn–O3}) = 1.942$ Å, $d(\text{Zn–O2}) = 2.487$ Å, $d(\text{Zn–N1}) = 2.079$ Å, and $d(\text{Zn–N2}) = 2.078$ Å. Notice that the value of $d(\text{Zn–O2})$ is much larger than $d(\text{Zn–O1})$ and $d(\text{Zn–O3})$, indicating that the interaction between Zn and O2 is very weak. Each PABA ligand is bound to two zinc centers and each zinc atom is bound to four ligands. Thus, **1** adopts a 3D supramolecular structure. The packing of the molecule diagram of the crystal is shown in Fig. 2. It can be clearly seen that Zn^{II} centers are bridged by the PABA molecules with –COOH and –NH₂ groups. PABA, acting as bridging ligands as well as coordinate ligands, adopt different coordination mode to form the 3D structure. The 3D structure is further stabilized by N–H \cdots O, O–H \cdots O hydrogen bonding and π – π stacking interactions with N2–O4 distance is 2.871, and centroid-to-centroid distance are 3.784 and 3.809 Å, respectively [19]. Additionally, it can be seen from Fig. 2 that the resulting 3D coordination polymer has cavities formed along the crystallographic *a*-axis. Guest H₂O molecules locate in the cavities and form hydrogen-bonding interactions with adjacent carboxylic oxygen atoms ($d(\text{O2–O01}) = 2.885$ Å).

3.2. Removal of guest molecules: TGA and XRD studies

The X-ray single-crystal structure clearly indicates that cavities occupied by guest H₂O molecules along the *a*-direction exist in **1**. We were intrigued by the possibility of generating a porous framework by removing the guest H₂O molecules. Thus, thermal stability of compound **1** was investigated. Fig. 3 shows the DSC/TGA

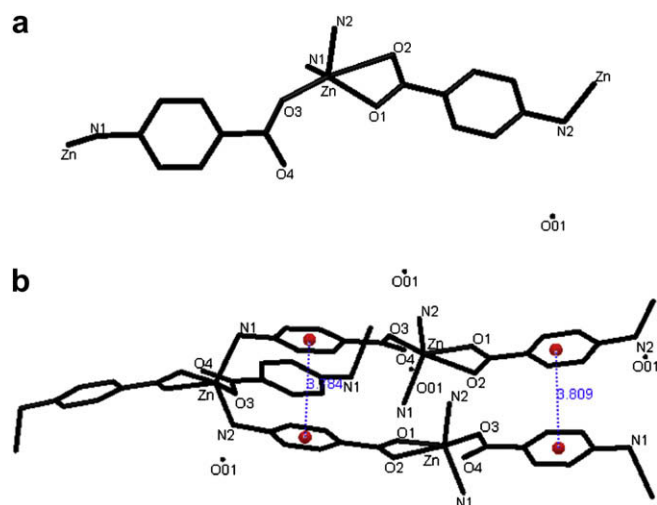


Fig. 1. Asymmetric unit of **1**(a) and coordination environment of zinc^{II} (b) (hydrogen atoms omitted for clarity).

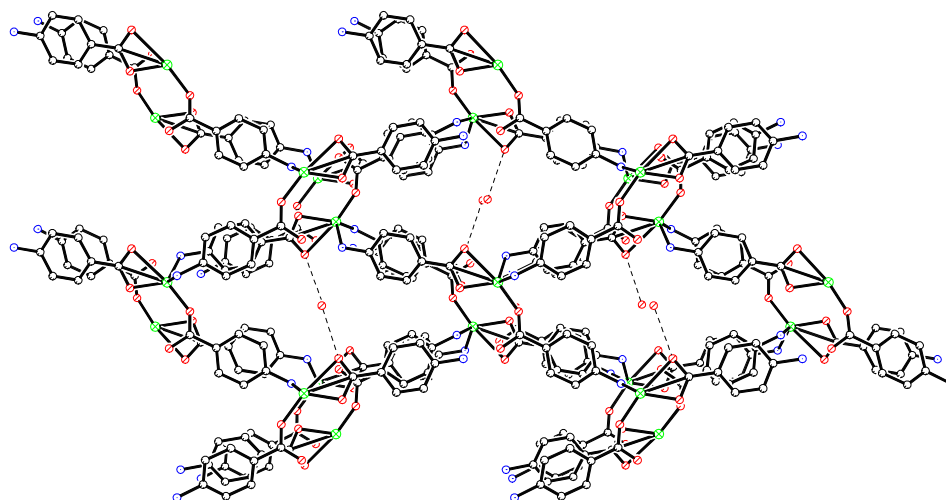


Fig. 2. Crystal packing of **1** viewed along the *a*-axis. Dashed lines represent the hydrogen bondings.

graph of complex **1**. The first weight loss of 6.94% from 30 to 136 °C corresponds to the loss of the guest H₂O molecule (calculated: 5.06%). There is no weight loss in TGA curve from 136 to 295 °C, but there is a distinct endothermic peak in the DSC curve, indicating that there is a phase transition process in the temperature range. Finally, the weight loss at 295 °C is due to the decomposition of the complex.

According to the DSC/TGA results, removal and reintroduction of guest H₂O molecules experiments were carried out and monitored by XRD. Compound **1** (33 mg) was placed inside an oven at 110 °C under vacuum. After 2 h, the sample exhibited a weight loss of 2.2 mg, equivalent to the loss of one H₂O molecule per formula unit (calculated, 1.67 mg). As shown in Fig. 4(c), after the removal of the H₂O molecules, the slight shift of some peaks may be attributed to the subtle change of the relative positions of some atoms in the crystal lattice [20]. Moreover, the guest H₂O molecules can be reintroduced into the evacuated sample of **1** by exposure to vapors atmosphere at room temperature for 24 h, which can be confirmed by powder XRD pattern (Fig. 4d) and DSC/TGA analysis (Fig. S1).

3.3. Second-harmonic generation

We measured the relative second-harmonic generation (SHG) activity of compound **1** using the Kurtz powder technique [21].

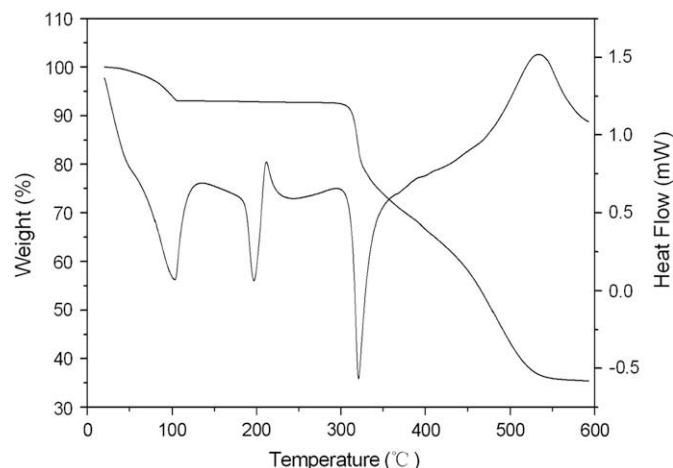


Fig. 3. DSC/TGA graph of complex **1**.

Pulse energy of 4 mJ/pulse, pulse width of 10 ns, and repetition rate of 10 Hz are used. Powdered samples of standard KDP and compound **1** with the same particle size were considered for powder SHG measurements. It was found that the SHG efficiency of **1** is equivalent to KDP crystal.

Furthermore, the SHG efficiency of compound **1** after removal and reintroduction of the guest H₂O molecules were measured. The SHG efficiency is decreased obviously after removal of the guest H₂O molecules. And it can come back when the H₂O molecules were reintroduced into the framework. This can be attributed to the two following reasons. (a) When the H₂O molecules were removed, the relative positions of some atoms in the crystal lattice may be changed to a certain extent. (b) The hydrogen bonding between H₂O molecules and carboxylic oxygen atoms may have more contribution to the SHG efficiency [22–25]. So, the SHG efficiency decreased with the removal of the H₂O molecules.

In summary, 3D coordination polymer [Zn(PABA)₂]·H₂O (**1**) has been synthesized under room temperature and structurally characterized. SHG efficiency of compound **1** was investigated by Kurtz powder technique, which indicated that the SHG efficiency of **1** is

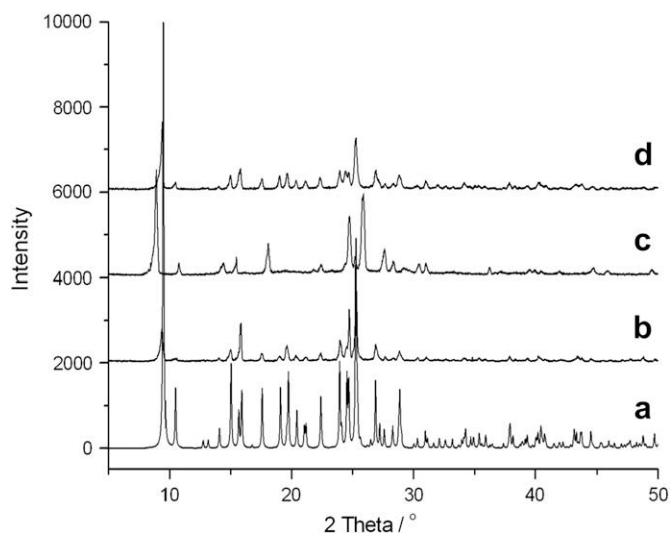


Fig. 4. Powder XRD patterns for **1**: (a) The simulated XRD pattern calculated from the single-crystal structure. (b) Taken at room temperature. (c) After removal of the guest H₂O molecules. (d) After reintroduction of the guest H₂O molecules.

equivalent to KDP crystal. The SHG efficiency is decreased obviously after removal of the guest H₂O molecules. And it can come back when the H₂O molecules were reintroduced into the compound. The present work also demonstrates that the framework of **1** is retained after removal of the guest H₂O molecules, indicating that this complex may also be used to generate porous materials.

Supporting information. Crystallographic data for the structural analysis have been deposited with the Cambridge Crystallographic Data Center, CCDC No. 684165. These data can be obtained free of charge from the Cambridge Crystallographic Data Centre via www.ccdc.cam.ac.uk.

Appendix. Supplementary data

Fig. S1. DSC/TGA graph of the complex, a) after the removal of guest H₂O molecules, b) after H₂O molecules were reintroduced into the framework.

Supplementary data associated with this article can be found in the online version, at [doi:10.1016/j.solidstatesciences.2009.02.005](https://doi.org/10.1016/j.solidstatesciences.2009.02.005).

References

- [1] S. Kitagawa, R. Kitaura, S.-i. Noro, *Angew. Chem., Int. Ed.* 37 (1998) 1460.
- [2] S. Kitagawa, R. Kitaura, S.-i. Noro, *Angew. Chem., Int. Ed.* 43 (2004) 2334.
- [3] B. Moulton, M.J. Zaworotko, *Chem. Rev.* 101 (2001) 1629.
- [4] B. Kesanli, W.B. Lin, *Coord. Chem. Rev.* 246 (2003) 305.
- [5] L. Pan, M.B. Sander, X. Huang, J. Li, M. Smith, E. Bittner, B. Bockrath, J.K. Johnson, *J. Am. Chem. Soc.* 126 (2004) 1308.
- [6] M. Fujita, J.Y. Kwon, S. Washizu, K. Ogura, *J. Am. Chem. Soc.* 116 (1994) 1151.
- [7] G. Tian, G.S. Zhu, X.Y. Yang, Q.R. Fang, M. Xue, J.Y. Sun, Y. Wei, S.L. Qiu, *Chem. Commun.* (2005) 1396.
- [8] R. Natarajan, G. Savitha, P. Dominiak, K. Wozniak, M. Narasimha, *J. Chem. Int. Ed.* 44 (2005) 2115.
- [9] D.B. Cordes, L.R. Hanton, M.D. Spicer, *Cryst. Growth Des.* 7 (2007) 328.
- [10] Y.L. Fur, R. Masse, *Acta Crystallogr., Sect. C* 52 (1996) 2183.
- [11] H.J. Chen, X.M. Chen, *Inorg. Chim. Acta* 329 (2002) 13.
- [12] R.H. Wang, M.C. Hong, J.H. Luo, F.L. Jiang, L. Han, Z.Z. Lin, R. Cao, *Inorg. Chim. Acta* 357 (2004) 103.
- [13] S.L. Zheng, M.L. Tong, X.L. Yu, X.M. Chen, *J. Chem. Soc., Dalton Trans.* (2001) 586.
- [14] H.L. Sun, C.H. Ye, X.Y. Wang, J.R. Li, S. Gao, K.B. Yu, *J. Mol. Struct.* 702 (2004) 77.
- [15] G. Smith, D.E. Lynch, C.H.L. Kennard, *Inorg. Chem.* 35 (1996) 2711.
- [16] R.H. Wang, M.C. Hong, J.H. Luo, R. Cao, Q. Shi, J.B. Weng, *Eur. J. Inorg. Chem.* (2002) 2904.
- [17] S.R. Marder, D.N. Beratan, L.T. Cheng, *Science* 252 (1991) 103.
- [18] G.M. Sheldrick, SHELXS and SHELXL, Institut für Anorganische Chemie der Universität, Göttingen, Germany, 1998.
- [19] C. Janiak, *J. Chem. Soc., Dalton Trans.* (2000) 3885.
- [20] T.M. Reineke, M. Eddaoudi, M. Fehr, D. Kelley, O.M. Yaghi, *J. Am. Chem. Soc.* 121 (1999) 1651.
- [21] S.K. Kurtz, T.T. Perry, *J. Appl. Phys.* 39 (1968) 3798.
- [22] V.R. Thalladi, S. Brasselet, H.C. Weiss, D. Bla1ser, A.K. Katz, H.L. Carrell, R. Boese, J. Zyss, A. Nangia, G.R. Desiraju, *J. Am. Chem. Soc.* 120 (1998) 2563.
- [23] R.A. Metcalfe, E.S. Dodsworth, S.S. Fielder, D.J. Stufkens, A.B.P. Lever, W.J. Pietro, *Inorg. Chem.* 35 (1996) 7741.
- [24] V. Moliner, P. Escibano, E. Peris, *New J. Chem.* (1998) 387.
- [25] Y.R. Xie, R.G. Xiong, X. Xue, X.T. Chen, Z. Xue, X.Z. You, *Inorg. Chem.* 41 (2002) 3323.